PERGAMON

Vision Research 42 (2002) 1771–1784

Vision Research

www.elsevier.com/locate/visres

Separating the effects of response nonlinearity and internal noise psychophysically

Leonid L. Kontsevich *, Chien-Chung Chen, Christopher W. Tyler

Smith-Kettlewell Eye Research Institute, 2318 Fillmore Street, San Francisco, CA 94115, USA

Received 22 November 1999; received in revised form 29 January 2002

Abstract

A psychophysical method is proposed to separate the contrast dependence of internal response and its noise. The resulting contrast relationships represent a signature of the visual processing stage that limits the human observer's performance. The method was applied to contrast discrimination for sustained and transient Gabor patches with a 3 cycle/deg spatial carrier. For both stimulus types the predominant noise was found to be multiplicative with a power exponent of 0.76–0.85 and the source of this noise preceded by an accelerating signal transducer with a power of 2–2.7. These exponents combine to account for the classic compressive power of about 0.4 for the signal-to-noise ratio in contrast discrimination. The estimated transducer acceleration suggests that there is a direct computation of contrast energy in the visual cortex.

1. Introduction

Since the pioneering work of Swets (1961) and Tanner (1961), it has been widely recognized that discrimination between different strengths of sensory stimuli is limited by noise in the internal responses evoked by those stimuli. It would be natural to expect, then, that independent measurement of the signal and noise-related components in the internal response would be a core issue in neurophysiology and psychophysics. Despite a significant effort (Geisler & Albrecht, 1997; Snowden, Treue, & Andersen, 1992; Softky & Koch, 1993; Tolhurst, Movshon, & Dean, 1983; Vogels, Spileers, & Orban, 1989), neurophysiology has not provided a decisive answer because signal and noise characteristics differ between the visual processing stages and it remains unclear which neural stage is critical to the observer's performance. Determining this critical stage may be challenging since it may be different for different visual tasks. In psychophysics, theoretical analyses provided by Ahumada (1987) and Legge, Kersten, and Burgess (1987) have demonstrated that the effects of a transducer nonlinearity are psychophysically equivalent to the effects of an internal, signal-dependent noise, which led them to conclude that distinguishing between these effects would be impossible.

Derivation of this theoretical equivalence rests on an assumption of Green and Swets (1966) that the noise levels in the discrimination task are the same for both stimuli. This assumption is reasonable when the differences in test level are a fraction of the pedestal value; it easily can fail, however, when the differences to be discriminated are large (Tyler & Liu, 1996). Elaborating this notion, the present study introduces a novel approach for assessment of the respective nonlinearities in the internal response and its noise at the critical neural processing stage that limits psychophysical discrimination thresholds. This approach will be described in general terms and tested for the contrast dimension of visual stimulus strength.

Two previous attempts to dissociate signal and noise nonlinearities in the visual processing by psychophysical means, both of which suffer from circularity of their logic. The first was by Lu and Dosher (1999), who attempted to solve this problem with the equivalent noise paradigm and obtained results very similar to those described in our study. In their analysis, however, they make the critical assumption that the noise standard deviation is proportional to the signal, which has no experimental or theoretical justification. Another attempt was published by Gorea and Sagi (2001) while our paper was under revision. These authors claim that in

* Corresponding author. Tel.: +1-415-561-1793; fax: +1-415-561-1610/345-8455.

E-mail address: lenny@ski.org (L.L. Kontsevich).

0042-6989/02/$ - see front matter
PII: S0042-6989(02)00091-3

concurrent contrast discrimination tasks observers use the same criterion, and based on this claim they produce separate estimates for signal and noise nonlinearities. The problem with this approach is that the data provided do not isolate the unique criterion constraint among other possibilities. Both studies are reviewed in detail below.

2. The model

The observer model used in this study is shown in Fig. 1. The model is built around the concept of a *critical noise* locus which limits the performance of a particular psychophysical task. This concept is developed in full in Appendix A. Within the model framework, there are three components that determine observer's performance: sources of nonlinearity preceding the critical noise infusion, the variation of critical noise with contrast, and the decision stage. The response nonlinearity is assumed to be monotonic (see Appendix A). In a two-alternative forced-choice (2AFC) task, the decision mechanism compares the two stimuli based on their responses and chooses the stronger one. Any nonlinearity that may follow the critical stage is omitted because it has no effect on the observer's performance (Birdsall's theorem). The other (noncritical) noise sources are also omitted because, as we show, they are likely to have a negligible effect. It should be noted that the critical noise source may vary among different stimuli and tasks, and, therefore, the nonlinearity preceding it would also vary. In particular, if the dominant noise is external, such as quantal or stimulus noise, there should be no nonlinear stage in the model.

The reader might notice that our specification does not incorporate a contrast gain-control stage. We omitted this feature because the analysis and the data to be presented will be limited to the contrast discrimination task, where the mask has the identical spatial and temporal profile to the test increment. In this context, any contrast gain control can be safely treated as an intrinsic component of the signal transducer.

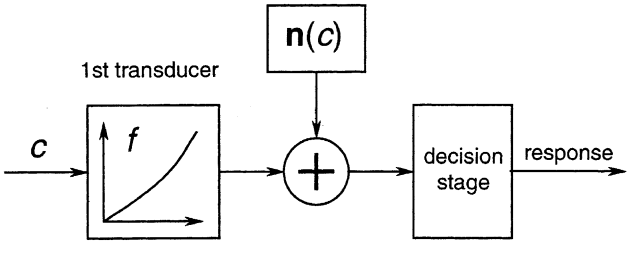

Fig. 1. The nonlinear transducer model employed in the paper. Noise preceding and following the critical noise $\mathbf{n}(c)$ may be neglected. Any nonlinear signal transducer that follows the critical noise stage may be omitted since it does not affect the results of a 2AFC experiment. The critical noise may depend on response strength.

3. Discrimination thresholds

The model is specified for contrast discrimination thresholds measured with the 2AFC paradigm (Foley, 1994; Greenlee & Heitger, 1988; Legge, 1981; Legge & Foley, 1980; Ross & Speed, 1991; Wilson & Humanski, 1993). When the input stimulus has contrast c, the response at the critical stage is a random variable, which can be expressed as the sum of two contrast dependent factors

$$\mathbf{r}(c) = f(c) + \mathbf{n}(c), \tag{1}$$

where f is the transducer preceding the critical stage and $\mathbf{n}$ is the noise at the critical stage. If, in a 2AFC trial, two stimuli with contrasts c (reference stimulus) and $c + \Delta c$ (test stimulus) are compared, the probability for the test stimulus to appear stronger than the reference can be expressed as

$$p(\text{test} > \text{reference}) = p(\mathbf{r}(c + \Delta c) > \mathbf{r}(c)) \tag{2}$$

or, substituting for $\mathbf{r}$ in Eq. (2) from Eq. (1) and expressing the result in terms of the cumulative density function (CDF) of the difference between noise components,

$$\begin{aligned} p(\text{test} > \text{reference}) &= p(f(c + \Delta c) + \mathbf{n}(c + \Delta c) \\ &> f(c) + \mathbf{n}(c)) = p(\mathbf{n}(c) - \mathbf{n}(c + \Delta c) \\ &< f(c + \Delta c) - f(c)) \\ &= P_{\mathbf{n}(c)-\mathbf{n}(c+\Delta c)}(f(c + \Delta c) - f(c)), \end{aligned} \tag{3}$$

where P stands for the CDF of the random variable shown in the subscript.

As in previous analyses of the 2AFC paradigm (Foley & Legge, 1981; Green & Swets, 1966) the random variable $\mathbf{n}(c) - \mathbf{n}(c + \Delta c)$ is postulated to have a Gaussian distribution. There are two factors that make this assumption highly plausible. First, as was noted by Green and Swets (1966), if any (even very limited) pooling at the critical stage is present, the independent noise instances from different spatial/temporal loci are pooled together and tend to a normal distribution, as required by central limit theorem (Bain & Engelhardt, 1987). Second, if the noise distribution is skewed, the subtraction operation in $\mathbf{n}(c) - \mathbf{n}(c + \Delta c)$ cancels the skewness of the components making the resultant distribution more symmetrical and, therefore, closer to Gaussian. (When the distributions for $\mathbf{n}(c)$ and $\mathbf{n}(c + \Delta c)$ are identical, the difference distribution is inherently symmetrical.)

Incorporating the Gaussian assumption, Eq. (3) can be re-written in the following form:

$$p(\text{test} > \text{reference}) = \Phi\left(\frac{f(c+\Delta c) - f(c)}{\sqrt{[\sigma(c+\Delta c)]^2 + [\sigma(c)]^2}}\right), \quad (4)$$

where Φ stands for the Gaussian CDF with unity variance (which introduces the normalization term in the denominator) and $\sigma(c)$ is the standard deviation of noise $\mathbf{n}(c)$. The argument of the CDF on the right of Eq. (4) is conventionally expressed in terms of the discriminability parameter d', which is traditionally defined as signal-to-noise ratio for the additive noise case (Green & Swets, 1966; Tanner & Birdsall, 1958). For arbitrary noise we define discriminability d' as

$$d' \equiv \sqrt{2}\frac{f(c+\Delta c) - f(c)}{\sqrt{[\sigma(c+\Delta c)]^2 + [\sigma(c)]^2}} \quad (5)$$

(there are two variances under the square root sign, which necessitates the $\sqrt{2}$ multiplier in this definition). Discriminability is frequently defined as the distance between test and reference signals, which would require absolute values in the numerator of Eq. (5). We propose that this restriction is unnecessary, and our definition is more convenient when both increments and decrements are analyzed together. For the experimental paradigm discussed, discriminability can be computed as

$$d' = \sqrt{2}\Phi^{-1}(p(\text{test} > \text{reference})), \quad (6)$$

thus providing the link between model and experiment.

We are now ready to derive a formula for discrimination threshold. Let the discrimination threshold Δc_{thr} be defined by $d' = 1$, which corresponds to $\Phi(1/\sqrt{2})$, which, in turn, translates to the 76% correct level:

$$\frac{f(c+\Delta c_{\text{thr}}) - f(c)}{\sqrt{[\sigma(c+\Delta c_{\text{thr}})]^2 + [\sigma(c)]^2}} = \frac{1}{\sqrt{2}}. \quad (7)$$

For arbitrary functions f and σ there is no closed-form solution for Δc_{thr}. However, when the reference contrast c exceeds a few detection thresholds, the experimental discrimination thresholds are typically much smaller than the reference contrast, the first-order approximation of Eq. (5) allowing to be used

$$d' \approx \frac{\mathrm{d}f(c)/\mathrm{d}c}{\sigma(c)}\Delta c. \quad (8)$$

This approximation leads to a closed-form solution for the threshold value Δc_{thr}:

$$\Delta c_{\text{thr}} = \frac{\sigma(c)}{\mathrm{d}f(c)/\mathrm{d}c}. \quad (9)$$

Thus, the discrimination threshold is proportional to the standard deviation of the noise distribution and is reciprocal to the first derivative (instantaneous gain) of the transducer at the reference contrast level. Note that this expression requires explicit knowledge of both the response and its noise, and cannot be derived solely from the response-to-noise ratio f/σ.

It is worth mentioning that the standard analysis of discrimination thresholds measured with the 2AFC paradigm (e.g., Foley & Legge, 1981) restricts the test-reference difference Δc to non-negative values because the probability measure of correct responses adopted in this paradigm cannot be <0.5. In our analysis, the equations derived (Eqs. (2)–(6)) do not have such a constraint because the probability measure $p(\text{test} > \text{reference})$ varies across the full range from 0 to 1: $p(\text{test} > \text{reference}) > 0.5$ for positive Δc and $p(\text{test} > \text{reference}) < 0.5$ for negative Δc. The measured probability range, therefore, doubles that measured by the standard one for the 2AFC procedure, providing additional information about underlying processes.

4. Parametric model

The major unknown of the model proposed is how the signal $f(c)$ and noise $\sigma(c)$ are related to the stimulus contrast at high contrast levels. We postulate that both quantities are power functions of the stimulus contrast (Geisler & Albrecht, 1997; Gottesman, Rubin, & Legge, 1981; Stevens, 1957; Tolhurst et al., 1983).

We are free to choose the response units such that

$$f(c) = c^p, \quad (10)$$

that is, there is no gain-related multiplier in this formula. The noise power function is defined by a separate exponent q relative to the response

$$\sigma(c) = kf(c)^q = kc^{pq}, \quad (11)$$

where k sets the same units for the noise standard deviation as for the response. (Recall that $q = 0$ corresponds to additive noise and $q = 0.5$ corresponds to Poisson noise.) Given these parameterizations Eq. (4) can be re-written as

$$p(\text{test} > \text{reference}) = \Phi\left(\frac{(c+\Delta c)^p - (c)^p}{k\sqrt{(c+\Delta c)^{2pq} + c^{2pq}}}\right) \quad (12)$$

and Eq. (9) as

$$\Delta c_{\text{thr}} = (k/p)c^{1+pq-p}. \quad (13)$$

Eq. (13) provides a stringent test for the feasibility of the power approximations postulated by Eqs. (10) and (11), requiring a power function relationship between discrimination thresholds and reference contrast. Such a relationship, indeed, was empirically discovered by Legge (1981) and later confirmed in numerous studies. The power function exponent, i.e., $(1 + pq - p)$ in terms of the model, varies from 0.2–0.3 (Greenlee & Heitger,

1988; Wilson & Humanski, 1993; Wilson, McFarlane,& Phillips, 1983) to 1 (Bradley & Ohzawa, 1986; Kulikowski & Gorea, 1978) and higher (Greenlee & Heitger, 1988), with typical values clustering at around 0.5–0.7 (Legge, 1981; Legge & Foley, 1980; Nachmias & Sansbury, 1974; Ross, Speed, & Morgan, 1993; Wilson et al., 1983).

Discrimination thresholds, as follows from Eq. (13), impose two constraints on the three free parameters of the model, which provide values for the response-to-noise ratio exponent $p - pq$ and the fraction k/p. The values of the individual parameters, however, cannot be obtained with purely threshold data. Our next goal, therefore, is to find an additional constraint to resolve the individual parameter values.

5. Adding external noise does not produce new constraints

The equivalent noise paradigm, where a controlled amount of the external noise is equated with the noise inherent to the stimulus, is widely considered a powerful tool for assessing internal noise in the visual system. If this were correct, we could get a direct measure for the noise exponent q and then derive the transducer exponent p from the discrimination threshold exponent. This possibility, unfortunately, has been ruled out by Legge et al. (1987), who showed that the equivalent noise measure depends both on the noise in the system and the transducer nonlinearity. They demonstrated that a nonlinear system with external additive noise will behave in exactly the same way (within the accuracy of the first-order approximation) as a linear system with internal signal-dependent noise. Thus, adding external noise in the detection task does not provide new constraints to discriminate these alternatives.

There still remains the possibility that expanding the experimental task from detection to discrimination in presence of the external noise would produce the desired constraint. The analysis provided in Appendix B demonstrates that external noise is still incapable of disentangling response and noise nonlinearities.

6. An additional constraint for model parameters

So far, our attempts to constrain signal and noise nonlinearities have been limited to the range where the difference between test and reference is much smaller than the reference ($c \gg \Delta c$), as in most contrast discrimination experiments. Observer performance for this range can be faithfully described by first-order approximations for the model expressed by Eqs. (8) and (9). The failure to resolve signal and noise within the linear range suggests that we should assess observer performance $p(\text{test} > \text{reference})$ at larger differences between test and reference, where the model behavior becomes nonlinear. To test the feasibility of this approach, we evaluate the nonlinear behavior of the model by means of Eq. (5). The linear component of the model determined by Eq. (8) predicts a linear relationship presented between discriminability d' and contrast difference Δc. Any deviation from the straight line thus represents a nonlinear component of the model that may produce the desired constraint.

Sample d' functions were computed with the formula given by Eq. (5) for three kinds of the transducers: compressive ($p = 0.5$), linear ($p = 1$) and expansive ($p = 2$), and for three kinds of the Gaussian noise: additive ($q = 0$), Poisson-like multiplicative ($q = 0.5$) and linearly multiplicative ($q = 1$). The noise gain k was set at a realistic value of 0.25; the reference had a contrast $c = 0.3$ as in the experiments to be described below. The plots in Fig. 2 clearly indicate that the shapes of the d'-vs.-Δc curves depend on the values of the parameters p

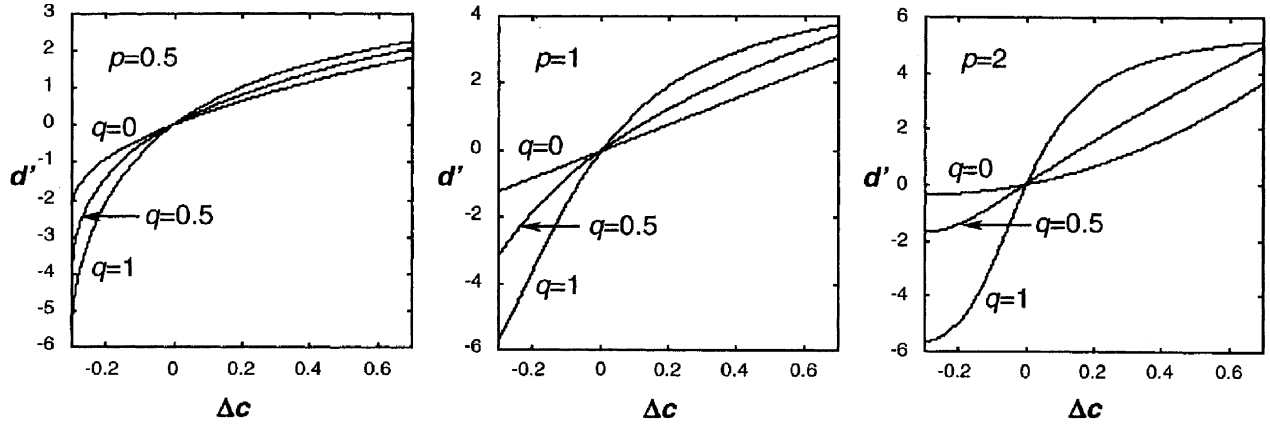

Fig. 2. The d'-vs.-Δc curves computed for a range of the transducer and noise power exponents p and q. These functions exhibit curvature whereas the first-order approximations analyzed so far predict straight lines. This curvature provides the nonlinear constraint critical to resolving the parameter values from the data.

and q, which may provide the missing constraint for estimating the values of the transducer nonlinearity. It is important to mention that the curve shapes are distinguishable within the readily measurable range of d' between -3 and 3, which corresponds to the range between 0.017 and 0.983 for the experimentally measured probability $p(\text{test} > \text{reference})$. These probabilities are assessable in an experiment consisting of a few hundreds of trials per condition.

There is, however, a factor complicating utilization of this finding. In 2AFC experiments, observers may occasionally press a wrong key by mistake ('finger error') or make a random guess because of a lapse of attention. The effect of the both kinds of errors leads to a symmetric contraction of the psychometric function toward the 0.5 level, as is encapsulated in the following formula:

$$p(\text{test} > \text{reference}|p_{\text{fe}}) = p_{\text{fe}} + (1 - 2p_{\text{fe}})p(\text{test} > \text{reference}|0), \quad (14)$$

where p_{fe} is the finger-error probability and $p(\text{test} > \text{reference}|0)$ assumes no finger errors and is computed according to Eq. (12). This contraction is also symmetric on the d' scale relative to the $d' = 0$ level, whereas the nonlinear distortion of d'-vs.-Δc curves in Fig. 2 are evidently asymmetric relative to the origin. Expressed in the terms of the Taylor series expansion, the effect of the finger errors appears only in the odd terms in the psychometric function leaving the even terms intact. On the other hand, the effect of the response and noise nonlinearities has a prominent even component. Since this even component is not present in the first-order approximations analyzed so far, it should provide a new nonlinear constraint for the model parameters. The simulation results indicate that this even component is quite large and within the measurable range.

Another potential cause for a discrepancy between the data and the model could be a deviation of the noise distribution from normality. In Appendix C we compared the observer's performance with the Gaussian internal noise postulated in our model and with Poisson noise, which is typical for neural spike generation processes. Extensive Monte-Carlo simulations show that these distributions produce indistinguishable results.

To conclude, we have demonstrated that, by measuring discrimination performance in the nonlinear regime (medium to large d' values), we gain a new constraint onto the model parameters. This constraint can be separated from the effects caused by 'finger errors' and attention lapses. Deviation of the noise distribution from normal to Poisson is shown to have minor, if any, effect on the results.

Next, we apply the proposed analysis to actual experimental data.

7. Experiment

7.1. Apparatus

The stimuli were presented on a 14 in. Sony monitor controlled by visual attenuator (Institute for Sensory Research, Syracuse University) and the Video Toolbox software (Pelli & Zhang, 1991) running on a PowerMac 604 computer with G3 accelerator. The monitor resolution was set at 640 by 480 pixels and the frame rate was 67 Hz; thus the duration of each frame was 15 ms. The monitor screen was viewed monocularly with the dominant eye from 136 cm distance, providing a resolution of $1'$ per pixel. Experiments were conducted in the dark.

7.2. Stimuli

The stimuli were Gabor grating patches defined according to

$$L = L_0[1 + c(t)\mathrm{e}^{-(x^2+y^2)/\sigma^2}\cos(2\pi fx + \varphi)] \quad (15)$$

with background luminance $L_0 = 30$ cd/m^2, Gaussian envelope size $\sigma = 2$ deg, and carrier spatial frequency $f = 3$ cycle/deg. The carrier phase φ was randomly chosen between 0 and 2π on each presentation to reduce local luminance adaptation and eliminate local luminance cues. Positional and spatial uncertainty introduced by the phase randomization should have no effect on our results since the stimulus contrasts were well above the detection threshold.

Two forms of temporal modulation for the contrast $c(t)$ were tested. The sustained stimuli had a raised cosine envelope $c(t) = c[1 - \cos(2\pi t/T)]$ with duration parameter $T = 500$ ms. The transient stimuli had the same envelope but their contrast was reversed every two frames, giving carrier frequency of 16 Hz.

7.3. Method

The experiments employed the constant stimulus method combined with a 2AFC paradigm. On each trial two stimuli, reference and test, were presented in random order. The observer's task was to choose the stimulus that had higher contrast by pressing one of two keys. There was also an option to repeat the trial, in which case the order in a new trial was chosen independently from the previous trial. Observers were asked to repeat a trial whenever they blinked or felt that they were not concentrating, to reduce the probability of the finger errors. Repeat rates were low, about 2 per hundred trials.

Contrast discrimination performance was estimated for three reference contrasts: 0.15, 0.3 and 0.6. For the reference contrasts of 0.15 and 0.6, the test stimuli always had a higher contrast than the reference. These conditions were run to constrain the d'-vs.-contrast exponent

and probability of the finger errors. For the 0.3 reference contrast, the test stimuli had both higher and lower contrasts to reveal an even nonlinear component in the psychometric function. All psychometric functions were measured with at least 200 trials per condition.

7.4. Observers

Two well-trained observers, AK (male), and SV (female), both high-school students, were employed in the experiments. The observers were naïve regarding the goal of the experiment, had normal (AK) and corrected to normal (SV) vision, and were paid for their work.

7.5. Results

The experimental results are shown in Fig. 3 on separate panels for each observer and each reference contrast. In all panels the psychometric functions become shallower for higher reference contrast with corresponding threshold increase. The experimental data are shown by circles, the lines represent the model fits.

8. Model fits

The data shown in Fig. 3 were fit by the model defined by Eqs. (12) and (14). The model had four free parameters: response and noise exponents p and q, noise gain k and finger error p_{fe}; its predictions were computed in accord with the formulae given in Eqs. (12) and (14). A multi-parameter optimization procedure for these parameters minimized the χ^2 error between the experimentally measured and predicted probabilities of correct.

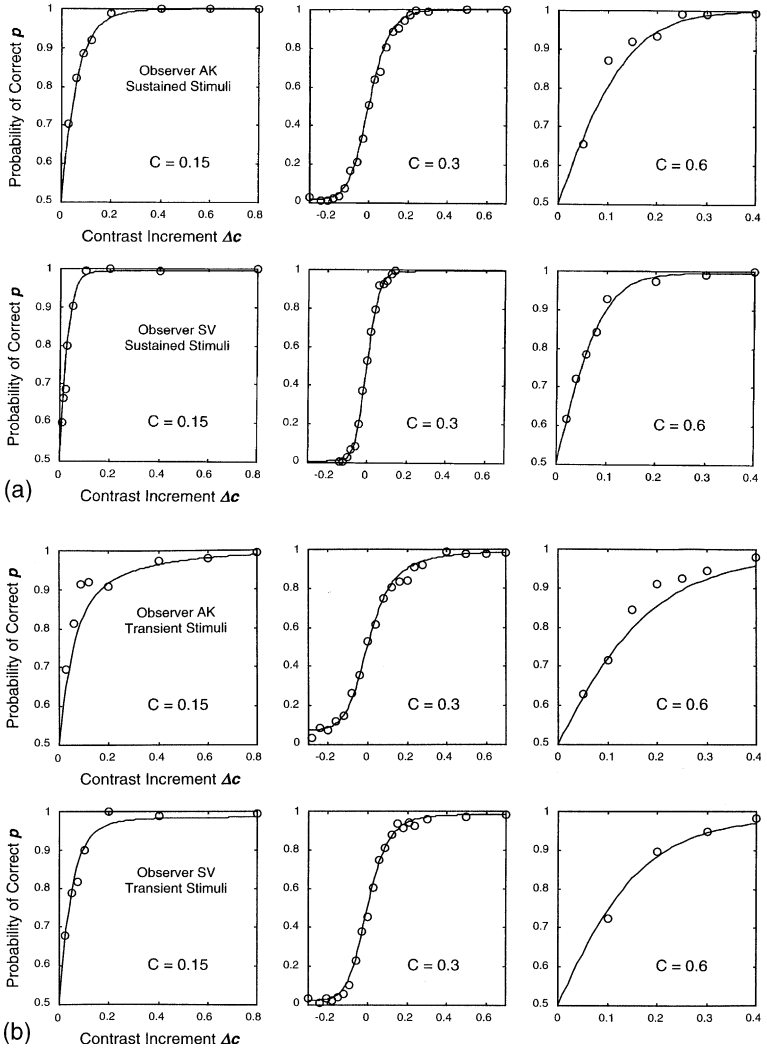

Fig. 3. The data for two observers and for sustained and transient stimuli. The curves represent fits of the optimized model. For the reference contrasts $c = 0.15$ and $c = 0.6$ performance was measured only for contrast increments ($\Delta c > 0$); for $c = 0.3$ both increments and decrements were evaluated.

The χ^2 error was computed based on variance of the model estimates (vs. variance of the experimental data). Suppose, that for a given stimulus condition (defined by c and Δc) the model predicts the probability P of correct responses, and an observer made m correct judgments in n trials. The probability of correct after n trials for the model observer would have binomial distribution with mean P and variance $P(1-P)/n$. The χ^2 error for that condition, therefore, can be computed as:

$$\chi^2(c,\Delta c)=\frac{(P-m/n)^2}{P(1-P)/n}. \tag{16}$$

The overall χ^2 error of the model fit across all conditions tested was the sum of χ^2 errors for each datum point.

An alternative way to compute χ^2 for a point would employ normalization by the variance of the experimental probability, which also has a binomial distribution with mean m/n and variance $m(n-m)/n^3$. The problem with this approach is that the variance falls to zero when observer responds correctly or incorrectly in all trials, i.e., $m=n$ or $m=0$, and putting such a variance in the denominator of Eq. (16) would leave χ^2 undefined. Conversly the ratio given by Eq. (16) is always defined regardless of the observer responses, given that model estimates for the probability of correct never reach the extreme values of zero and one. This method for computing of the χ^2 error is widely used for analysis of contingency tables, although it is typically expressed in terms of frequencies rather than probabilities.

The confidence intervals for optimized parameter values were estimated as proposed in Bevington and Robinson (1992, p. 212–214). As the first step, optimization for all four parameters provided the smallest possible χ^2 error. Then one of the parameters was fixed to a certain (nonoptimal) value and optimization for the remaining three was repeated. The χ^2 error in this case was, indeed, larger than the smallest one. Using the bisection method we found the values of fixed parameters where the χ^2 error increased by a value of 1 relative to the smallest χ^2. These two values for each parameter constituted a 68.3% confidence interval corresponding to one standard deviation of the normal distribution of the measurement error.

The optimized parameter values for two types of stimuli and for two observers are presented in Table 1. The 68.3% confidence intervals for all four optimized parameters are presented in parentheses below the optimal values. The next row shows the d'-vs.-contrast exponents, which are computed as $1+pq-p$, see Eq. (13). The next three rows present the optimal fit error χ^2, the number of the degrees of freedom, and the P value for the χ^2 random variable with the assigned number of degrees of freedom to exceed the estimate.

At a reviewer's request, P values for the fit of the linear transducer model with additive noise ($p=1$, $q=0$) are presented in the last row. The model was optimized with exponent parameters constrained and the number of the degrees of freedom increased by 2.

9. Discussion

The optimized parameters show remarkable consistency across the observers and the conditions. For only one condition (transient stimuli, observer AK) is the P value smaller than 0.05, suggesting that the model may not fit these data within the measurement error. As the confidence intervals show, most of parameter estimates are tightly constrained. To provide some intuition as to why these estimates are tight, we present in Fig. 4 the optimization results for pedestals $c=0.3$ in d'-vs.-Δc format. The smooth curves show the fit of the optimized model; the circles show the detectability values computed from the experimental data. The data points follow a similar pattern to the model predictions for $p=2$ and between 0.5 and 1 shown in the rightmost panel of Fig. 2 and obviously deviate from the predictions for smaller values of the response exponent p. The response exponent $p=2$ is close to the optimal values presented in Table 1. P values for all fits of linear transducer model with additive noise (last row of Table 1) are extremely small, which allows us to reject this model with high confidence.

Table 1
Model parameters estimated from the experimental data

Modulation	Sustained		Transient	
	Observer AK	Observer SV	Observer AK	Observer SV
k	0.23 (0.21, 0.25)	0.16 (0.08, 0.21)	0.41 (0.36, 0.44)	0.28 (0.21, 0.36)
p	2.3 (2.1, 2.5)	2.3 (1.1, 3.0)	2.7 (2.5, 2.9)	2.0 (1.5, 2.4)
q	0.76 (0.73, 0.79)	0.83 (0.60, 0.88)	0.85 (0.81, 0.87)	0.85 (0.78, 0.89)
p_{fe}	0 (0, 0.003)	0.011 (0.006,0.017)	0.003 (0, 0.03)	0.028 (0.016, 0.041)
Slope	0.44	0.60	0.58	0.70
χ^2	35.2	28.5	76.1	39.4
d.f.	31	27	27	32
P-value	0.28	0.39	1.5×10^{-6}	0.17
P-value for $p=1$, $q=0$	1.3×10^{-7}	4.7×10^{-14}	$<10^{-16}$	1.1×10^{-16}

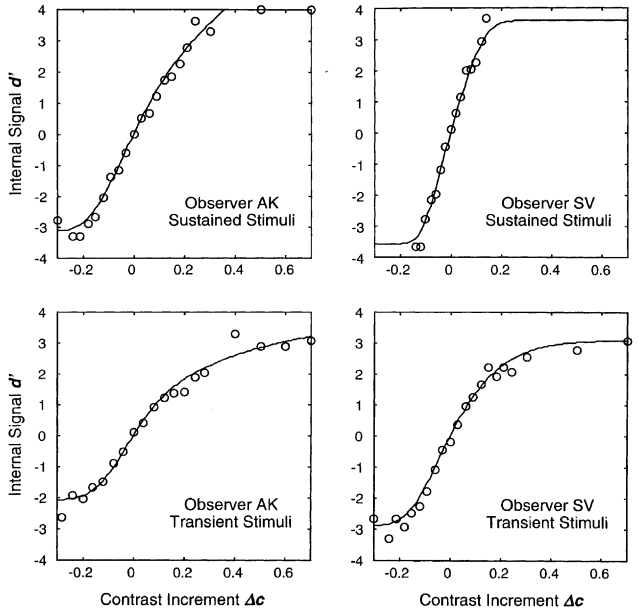

Fig. 4. The model fits for pedestal contrast $c = 0.3$ in d'-vs.-Δc format. The circles show the detectability computed from experimental data. The two rightmost circles in the upper-left plot are included for completeness; they have infinitely large d' instead of $d' = 4$ indicated. The curves represent fits of the optimized model.

These results will be analyzed from psychophysical point of view before considering the neurophysiological conditions.

9.1. Psychophysical analysis

The power exponent p for the response transducer fell within the range from 2 to 2.7 for both observers and both stimuli. This high exponent value would not be surprising if it were estimated for near-detection contrast levels (Foley & Legge, 1981; Legge, 1984; Stromeyer & Klein, 1974). Here, however, we evaluated the response transducer at higher contrasts where the transducer is widely believed to be saturating, which implies a transducer exponent of less than one (Gottesman et al., 1981; Wilson, 1980). At the same time, numerous studies have indicated that there is a stage in the visual processing pathway that computes contrast energy (e.g., Adelson & Bergen, 1985; Manahilov & Simpson, 1999; Thomas & Olzak, 1997; Watson & Solomon, 1999) across the whole range of contrasts. The most advanced models of contrast gain control also assume the exponent of contrast signal transducer to be in the range between 2 and 2.4 (Albrecht & Geisler, 1991; Foley, 1994; Heeger, 1992). Our study provides psychophysical confirmation for the existence of such a stage and indicates that the observers' performance (for the tasks studied) is limited by noise infused *after* the contrast energy is computed. The data also show that there is no significant difference in either the transducer nonlinearity or the multiplicative noise gain between sustained and transient conditions.

Interestingly, Lu and Dosher (1999) also find the signal transducer exponent to be close to 2.5 based on their modeling of data obtained in equivalent noise experiments. In their model they make the assumption that the exponent of the multiplicative component of the noise has unity value ($q = 1$), which inserts the necessary constraint to resolve the inherent ambiguity of equivalent noise data (see Appendix B). This assumed value for the multiplicative noise exponent is arbitrary, as there is no evidence for its validity. Moreover, this exponent value predicts a unity exponent (see Eq. (13)) for discrimination thresholds at high pedestal contrasts where the additive noise component becomes negligibly small. (Unfortunately, Lu and Dosher do not measure the discrimination threshold exponent in their study, but there is no obvious reason why it should be higher than the typical value of 0.6.) Thus, we attribute the similarity between the estimates obtained in our study and by Lu and Dosher (1999) to a mere coincidence.

Another example of an arbitrary constraint used to disambiguate signal and noise transducer exponents can be found in a recently published study by Gorea and Sagi (2001). They interpret their data as strong evidence that, in two concurrent discrimination tasks, observers developed a common criterion for both stimuli. This conclusion led them to estimate the signal and noise exponents at about $p = 0.58$ and $q = 0.15$ respectively, i.e., according to their analysis the signal transducer is strongly compressive and the noise is almost additive. Though this result does not strictly invalidate our estimates (since we estimate the exponents at the critical noise stage and they estimated the exponents at the decision stage), their approach actually fails to provide independent estimates for signal and noise transducers. The problem with their analysis is that it does not single out the unique criterion constraint on which their logic is based. Instead, their data demonstrate that the observers equate false alarm rates for the mixed stimuli, which is consistent with a unique criterion but also with an infinite family of criterion rules, of which the unique criterion rule as just one member. Translating the false alarm rate to a criterion level requires an unknown gain factor for each different pedestal contrast. When this factor is included in the analysis and applied to their data, the Gorea and Sagi design does not provide any additional constraint over what is already known from discrimination threshold data (Kontsevich, Chen, Verghese, & Tyler, in press).

Given the well-known result that the contrast response transducer is approximately quadratic at high contrasts, it would be parsimonious to suggest that this property holds through the whole range of contrasts including the lowest ones. This suggestion is consistent with the data on the exponent of the d'-vs.-contrast

relationship measured in detection tasks: at low test contrasts, any response-dependent (multiplicative) component noise is likely to be buried in the spontaneous neural activity, which constitutes a response-independent (additive) component, and the contrast response exponent would solely determine the d'-vs.-contrast relationship, which is known to be close to a value of two (Foley & Legge, 1981; Legge, 1984; Stromeyer & Klein, 1974). The notion of a square law for the response transducer also gains support from a binocular contrast summation study (Legge, 1984) and from modeling (Watson, 2000) of the detection thresholds for a representative set of stimuli (Carney et al., 1999).

Estimates for d'-vs.-contrast exponents are presented in Table 1 for reference. The exponents for the sustained stimulation (0.44 and 0.60) are close to those measured by Legge (1981) under quite similar conditions (0.62 and 0.55 for 2 cycle/deg, 200 ms contrast onset). The exponents for the transient stimuli (0.58 and 0.70), however, are discrepant from those measured by Kulikowski and Gorea (1978) for similar conditions (0.99 and 1.00 for 5 cycle/deg, 8 Hz). We attribute this discrepancy to their use of a long adaptation period (2 min) preceding each trial, which our study lacked.

Integrating the results of the present study and the classic psychophysical studies on the transducer at low contrast levels, we argue that:

(a) contrast response at the critical stage for both detection and discrimination has a power of approximately 2.4 across the whole range of contrasts;
(b) the contrast-dependent multiplicative noise component is prominent at high contrasts, whereas at low contrasts the cortical noise is additive, being dominated by contrast-independent spontaneous neural activity.

We should mention that this analysis attributes the near-threshold nonlinearity solely to a transducer nonlinearity, thus, leaving no room for channel uncertainty effects (Pelli, 1985; Tyler & Chen, 2000) in typical detection tasks.

9.2. Neurophysiological analysis

Though our finding of transducer acceleration within the range 2–2.7 for the exponent p is unexpected for the domain of psychophysics, it is perfectly consistent with the neurophysiological data. The cells in the lateral geniculate nucleus (LGN) and visual cortex are known to have accelerating transducers, which may operate across the whole range of contrasts, or the range of low-medium contrasts, saturating at high-contrast range. A comparative study of the transducer exponents conducted by Sclar, Maunsell, and Lennie (1990), for example, shows that exponent values increase at each stage of visual processing. While the exponent is as small as 1.2 for magnocellular LGN and 1.6 for parvocellular LGN, it becomes 2.4 in V1, and 3 in MT (see their Table 1). Our estimates are close to the exponent found in V1, which would suggest that the critical stage for contrast discrimination is located either in V1 or in neighboring areas.

Additional evidence that the critical stage cannot be situated before V1 comes from the analysis of intracellular recordings of simple cells in cat (Jagadeesh, Wheat, Kontsevich, Tyler, & Ferster, 1997; Kontsevich, 1995). The nonlinearity exponents for intracellular recordings in simple cells lag in the range 0.7–1.4, i.e. far below the critical-stage estimate.

It should be mentioned that our placement of the critical stage in contrast processing in V1 or some area close to it and preceding MT is a plausible but not definitive conclusion, because direct comparison between the system as whole and individual cells may not be valid. Contrast response functions of cortical cells are known to be quite heterogeneous, and the behavior of a whole system may have different parameters than those of the individual components constituting it. One way to unify the mechanisms for contrast processing is to assume some normalization process that makes the neurons in the most sensitive part of their response range dominate the overall system response (Geisler & Albrecht, 1997). Such a scheme for "sewing" the individual contrast responses into a seamless function would resolve the issue of heterogeneity of individual sensitivities. However, these issues of linking hypotheses between neurophysiology and psychophysics are best left to the neurophysiologists to develop. Our goal is to define the performance of the human visual system as completely as possible, not to account for the behavior of all the neurons of which it is constituted.

The estimate of the power exponent q for the noise transducer fell in a narrow range between 0.76 and 0.85 across the observers and the stimuli. This result implies that the noise critical for contrast discrimination is infused after the quantal (Poisson) noise, which is effectively additive at a given mean luminance level. Our noise exponents also place the critical stage after the ganglion cell level, where the neural noise has similarly been shown to be additive relative to contrast (Croner, Purpura, & Kaplan, 1993). Our exponents, though, are in line with the experimental measurements of fluctuations in neural activity (Cohn, Green, & Tanner, 1975; Geisler & Albrecht, 1997; Snowden et al., 1992; Softky & Koch, 1993; Tolhurst et al., 1983; Vogels et al., 1989), which place the multiplicative noise exponents in the range between 0.5 and 0.75, ours being close to the upper bound of this range. We argue that the noise limiting our tasks has cortical nature and its source is located after the simple cells because the intracellular responses of simple cells appear to have linear

transducers in the studied range of contrasts (e.g., Kontsevich, 1995) whereas the psychophysical transducer is more than quadratic.

10. Conclusions

We have developed a technique for functional isolation of the separate signal and noise transducer behaviors for suprathreshold stimuli. The results show a strong multiplicative nonlinearity controlling the noise behavior. The signal transducer, rather than being estimated as compressive, exhibits an accelerating form. The accelerating power exponent of the signal transducer for these suprathreshold conditions is about 2.4, suggesting that the visual system computes something like contrast energy at the critical stage of visual processing. The predominant noise for the contrast discrimination task is then infused into that contrast energy signal by some contrast-dependent process with an exponent of about 0.8.

Appendix A

A general model for observer performance is shown in Fig. 5(a). The response evoked by a visual stimulus passes through a number of stages. Each (ith) stage is specified by its transducer function f_i and injected noise $\mathbf{n}_i$. Each noise component in this scheme may be contrast-dependent. External noise $\mathbf{n}_0$ in this scheme precedes all the processing stages. The internal response arriving at the decision stage (i.e., after all transducer stages) accumulates distortions from all previous stages:

$$\mathbf{r} = f_K(\ldots f_1(c + \mathbf{n}_0) + \mathbf{n}_1 \ldots + \mathbf{n}_{K-1}) + \mathbf{n}_K, \qquad (A.1)$$

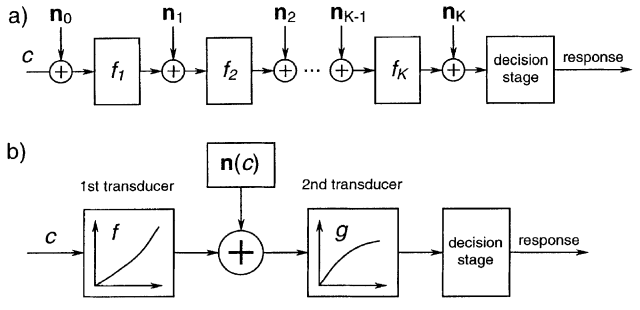

Fig. 5. Two models of the observer performance. In the most general model (a) the signal passes through of a number of the stages specified by transducer function f_k and injected noise $\mathbf{n}_k$. Each transducer can be nonlinear and each noise component in this scheme may be contrast-dependent. External noise $\mathbf{n}_0$ in this scheme precedes all the processing stages. The decision stage receives a signal that combines all the transducers and noise sources. If one of the noise sources is predominant, other noise sources can be neglected and the transducers can be collapsed into two, as in (b). According to Birdsdall's Theorem, the second transducer does not alter the decision in 2AFC trial and can be removed, as in Fig. 1.

where c is the stimulus contrast and K is the total number of stages. In contrast discrimination tasks at high contrast levels, the noise standard deviation is typically small relative to the response. This property allows a first-order approximation, i.e., the first term of the Taylor expansion to be used. After applying these linear approximations to Eq. (A.1), we arrive at the following approximation formula for the response $\mathbf{r}$:

$$\mathbf{r} \approx f_K(f_{K-1}(\ldots f_1(c)\ldots)) + w_0(c)\mathbf{n}_0 + w_1(c)\mathbf{n}_1 + \cdots + w_K(c)\mathbf{n}_K, \qquad (A.2)$$

where $w_i(c)$ is the contrast-dependent gain for the ith noise component. Assuming statistical independence between the noise sources, the standard deviation of the response at the decision stage is

$$\sigma_{\mathbf{r}} = (w_0^2\sigma_0^2 + w_1^2\sigma_1^2 + \cdots + w_K^2\sigma_K^2)^{1/2}. \qquad (A.3)$$

The quadratic sum in the right-hand side of Eq. (A.3) will tend to be dominated by the largest component. For example, adding an extra noise with a σ of half that of the critical noise increases the σ of the compound noise by only 12%. There, indeed, remains some possibility that many smaller noise sources could overwhelm the strongest one. Also for different stimulus contrasts the critical stages may be different. However, in the present study we assume that the noise in the internal response at the decision stage is dominated across the high-contrast range by only one noise source, which we call the *critical noise*.

Given this assumption, the other (noncritical) noise sources may be neglected and all nonlinear stages can be collapsed into two (one before and the other after the critical noise source), as shown in Fig. 5(b). An input signal, which is set by the stimulus contrast, passes through the first nonlinearity, after which noise is introduced into the signal, which then passes through the second nonlinear stage. It should be noted that the nonlinear stages implicitly incorporate spatial and temporal integration of the stimulus, which determine the values of the weight coefficients in the Eq. (A.2).

The nonlinear transducers in this model are assumed to be monotonic, that is, increase of input contrast always leads to increase of the internal response at intermediate and decision stages. If this were not the case, stimuli of different contrasts could produce the same internal response and would be indiscriminable as shown in Fig. 6. Such a result is atypical for the psychophysical literature on contrast detection and discrimination, however.

An important consequence of monotonic transducer assumption is that performance in a psychophysical experiment should not depend on the second transducer of the model depicted in Fig. 5(b). This notion, known as Birdsall's Theorem (Lasley & Cohn, 1981; Pelli, 1991), can be justified by the following argument. Consider a

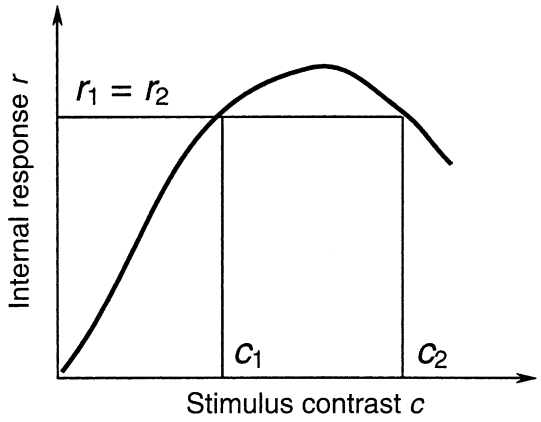

Fig. 6. If the transducer in the visual system were not monotonic, as shown by the curved line, there should exist different contrasts (c_1 and c_2), which produce the same responses and, therefore, indistinguishable. Such behavior is unknown for contrast discrimination tasks.

2AFC trial where an observer has to compare two stimuli with contrasts c_1 and c_2. The responses at the output of the first nonlinear transducer f are two values determined by the stimuli contrasts: $f(c_1)$ and $f(c_2)$. Then, after noise infusion, the responses become $f(c_1) + n_1$ and $f(c_2) + n_2$, where n_1 and n_2 are two instances of the noise random variable $\mathbf{n}(c)$. These noisy responses pass through the second nonlinear transducer g, producing the output responses to be compared by the decision stage are given by the following expressions: $g(f(c_1) + n_1)$ and $g(f(c_2) + n_2)$. The judgment made at the decision stage is based on the values of these responses: if the first response is greater than the second then the first stimulus will be selected as having higher contrast, and vice versa. Since transducer g is monotonic, the order relationship between its output values is identical to the order of its input values $r_1 = f(c_1) + n_1$ and $r_2 = f(c_2) + n_2$. Therefore, if the decision stage were located immediately after the critical noise infusion and compared r_1 and r_2, it would produce exactly the same judgment as one located after the second (monotonic) transducer. As a result, the second nonlinear transducer is transparent to a psychophysical experiment assessing probabilities of the correct responses and can be safely removed from the model, which leads to the final version shown in Fig. 1.

To summarize, the components of the model that may affect the outcome of a 2AFC experiment are the critical noise and the compound of nonlinearities preceding the critical noise infusion. Subsequent nonlinearities are transparent for the 2AFC task and can be ignored in this application (although they would affect the perceived contrast of the target).

This result has a corollary, which will be employed for analysis of the equivalent noise paradigm. When external (pattern) noise dominates over the internal (neural) noise, the critical stage shifts to the noise-infusion point $\mathbf{n}_0$, i.e., to the very beginning of the processing chain shown in Fig. 5(a). In this situation the outcome of a trial in a contrast discrimination experiment becomes independent of the nonlinear properties of the transducer and of any noise in visual system.

Appendix B

This Appendix presents a novel analysis of external noise effects in the contrast discrimination task. Previously, Legge et al. (1987) demonstrated that combining external noise with the detection task (as known as the equivalent noise paradigm) does not allow response and noise nonlinearities to be disentangled. There remains the possibility, though, that expanding the experimental task from contrast detection to contrast discrimination could provide an additional constraint for distinguishing response and noise nonlinearities. The discrimination task might also be a better match to our objective since, unlike the detection task, it would allow probing of high contrasts, the range of concern in the present study. As we show below, however, combining the contrast discrimination task with external noise fails to provide an additional constraint on response and noise nonlinearities beyond that available from a standard contrast discrimination task with no external noise added.

In the contrast discrimination paradigm, the effect of external noise can be conceptualized as additional contrast variability of the reference and test stimuli. The magnitude of this variability is proportional to the noise contrast and depends on the spatio-temporal properties of the noise and the receptive field of the critical stage. For example, a fine-grain noise will produce smaller variability in a large receptive field than in small one because of spatial averaging over the local fluctuations. Let the gain coefficient k_{ext} relate the external noise contrast c_{ext} to the standard deviation σ_{ext} of the response variability: $\sigma_{\text{ext}} = k_{\text{ext}} c_{\text{ext}}$. At high response levels, the output gain for external noise through a nonlinear transducer is defined by the first derivative pc^{p-1} of the nonlinear transducer function c^p, as shown in Fig. 7. Hence, the standard deviation of the external noise after the nonlinearity is equal to $pc^{p-1}\sigma_{\text{ext}}$. For the combined noise at that stage, the standard deviation σ_{sum} is given by the Euclidean norm:

$$\sigma_{\text{sum}} = \sqrt{(kc^{pq})^2 + (k_{\text{ext}} p c^{p-1} c_{\text{ext}})^2}. \tag{B.1}$$

The signal is given by the difference between the responses produced by the test and reference stimuli. For small values of Δc, which are typical for studies concerned with experimental threshold measurements, the first-order approximation is

$$(c + \Delta c)^p - c^p \approx p c^{p-1} \Delta c. \tag{B.2}$$

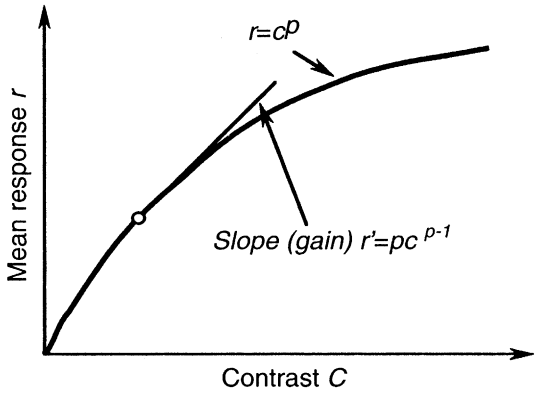

Fig. 7. The instant gain of the nonlinear transducer is defined by its first derivative.

The probability of choosing test $p(\text{test} > \text{reference})$ is determined by the discriminability (see Eq. (8))

$$d' \approx \frac{pc^{p-1}\Delta c}{\sqrt{(kc^{pq})^2 + (k_{\text{ext}}pc^{p-1}c_{\text{ext}})^2}}. \tag{B.3}$$

Suppose that we conduct a series of experiments where we measure $p(\text{test} > \text{reference})$ for a range of conditions defined by c, Δc, and c_{ext}. Are these data sufficient to constrain parameters p and q? The following counter-example demonstrates that the answer is negative.

Suppose that the parameters p, q, k, and k_{ext}, provide an exact fit to the data. Let us assign an arbitrary new value p' for the exponent of the transducer nonlinearity. Then, if q is replaced by $q' = (pq - p + p')/p'$ and k by $k' = kp'/p$, the value of the right-hand expression in Eq. (B.3) will remain exactly the same as its value for the original set of the parameters according to

$$\frac{pc^{p-1}\Delta c}{\sqrt{(kc^{pq})^2 + (k_{\text{ext}}pc^{p-1}c_{\text{ext}})^2}} \equiv \frac{p'c^{p'-1}\Delta c}{\sqrt{(k'c^{p'q'})^2 + (k_{\text{ext}}p'c^{p'-1}c_{\text{ext}})^2}}. \tag{B.4}$$

The only parameter that the data do constrain is k_{ext}. The value of the latter parameter reflects the sensitivity of the critical mechanism to a particular noise, which may be valuable for estimating the receptive field properties (see Legge et al., 1987; Solomon & Pelli, 1994). This paradigm, however, does not appear to be helpful for constraining the noise gain k or the nonlinearity exponents p and q.

Appendix C

To evaluate the sensitivity of the model predictions to deviations from the Gaussian noise assumption, we conducted extensive Monte-Carlo simulations of the model with Gaussian and Poisson noise. The latter was chosen as a possible candidate because it is thought to represent the neural spike-generation process.

For Gaussian noise the parameter values in the simulations were: $c = 0.5$ (a typical contrast value in a contrast discrimination experiment); $q = 0.5$ (a characteristic exponent for Poisson noise, otherwise the Gaussian noise would not behave comparably with the Poisson noise); $p = 0.5$, 1 and 2 (since we do not know the actual value); and $k = 0.1$ and 0.5 (the former value is typical in contrast discrimination experiments, the latter corresponds to an unrealistically high noise level to provide a stringent test of our model). The mean and standard deviation for Gaussian distribution were c^p and kc^{pq}, respectively, as specified in the model by Eqs. (10) and (11).

The Poisson noise distribution $p(x, \mu) = \mathrm{e}^{-\mu}\mu^x/x!$ is determined by a single parameter μ, which can be interpreted as the hypothetical number of spikes constituting the decision variable. To obtain the value of μ corresponding to a particular set of parameters defining the Gaussian distribution, we employed the property of the Poisson distribution that the ratio of its mean and standard deviation is equal to $\sqrt{\mu}$. The same ratio for the model with Gaussian noise is given by c^p/kc^{pq}. From the equality between these two expressions we obtain the following expression for μ:

$$\mu = c^{2p-2pq}/k^2. \tag{C.1}$$

Table 2 shows the μ values for all pairs of p and k tested in the simulations.

Estimates of an observer's performance were obtained with Monte-Carlo simulations of 100,000 experimental trials per condition. The results are shown in Fig. 8 by solid lines for the Gaussian noise distribution and by dashed lines for the Poisson distribution. In the left panel, which corresponds to the case of $k = 0.1$, both noise distributions produce identical results. This match is not surprising because at large μ values the Poisson distribution is indistinguishable from the Gaussian.

A critical test, therefore, is provided by the noise gain value $k = 0.5$, which takes the model to an unrealistic extreme where a stimulus with contrast $c = 0.5$ is represented by 1–3 spikes (depending on the nonlinearity exponent) at the decision level. The detection thresholds at this contrast are also unrealistically high: the discrimination threshold at 76% correct is at least as

Table 2
Values of Poisson parameter μ required to match the Gaussian model with parameters p and k

k	p		
	0.5	1	2
0.1	70.7	50	25
0.5	2.83	2	1

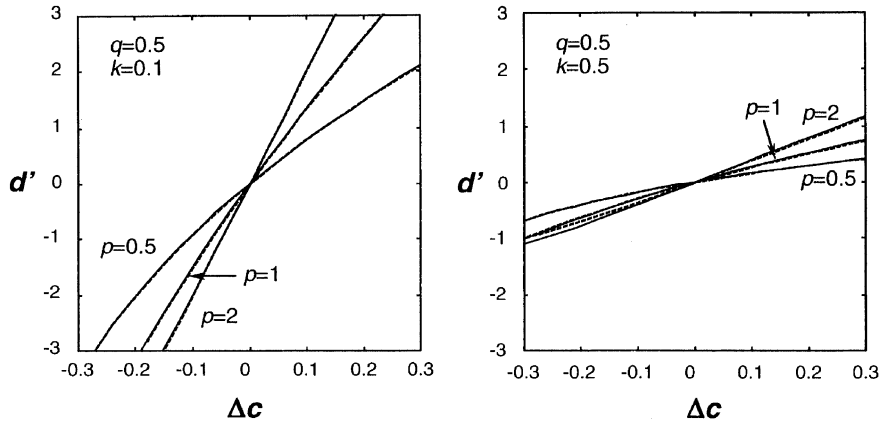

Fig. 8. Comparison of Monte-Carlo simulations of the observer performance for Poisson (dashed line) and Gaussian (solid line) noise. See text for details.

high as 0.25, i.e., the observer performance would be very poor in discriminating contrasts of 0.5 and 0.75. Nevertheless, in all cases the predictions for Poisson and Gaussian noise remain practically identical, which assures us that any deviation of the noise distribution from Gaussian toward Poisson should have a negligible effect on the results of our analysis.

References

Adelson, E. H., & Bergen, J. R. (1985). Spatiotemporal energy models for the perception of motion. *Journal of the Optical Society of America A, 2*, 284–299.

Ahumada, A. J., Jr. (1987). Putting the visual system noise back in the picture. *Journal of the Optical Society of America A, 4*, 2372–2378.

Albrecht, D. G., & Geisler, W. S. (1991). Motion selectivity and the contrast-response function of simple cells in the visual cortex. *Visual Neuroscience, 7*, 531–546.

Bain, L. J., & Engelhardt, M. (1987). *Introduction to probability and mathematical statistics*. Boston: Duxbury.

Bevington, P. R., & Robinson, D. K. (1992). *Data reduction and error analysis for the physical sciences* (second ed.). Boston: McGraw-Hill.

Bradley, A., & Ohzawa, I. (1986). A comparison of contrast detection and discrimination. *Vision Research, 26*, 991–997.

Carney, T., Klein, S. A., Tyler, C. W., Silverstein, A. D., Beutter, B., Levi, D., Watson, A. B., Reeves, A. J., Norcia, A. M., Chen, C.-C., Makous, W., & Eckstein, M. P. (1999). The development of an image/threshold database for designing and testing human vision models. *Proceedings, Human Vision, Visual Processing, and Digital Display IX* (pp. 542–551), SPIE, Bellingham, WA, 3644.

Cohn, T. E., Green, D. G., & Tanner, W. P., Jr. (1975). Receiver operating characteristic analysis. Application to the study of quantum fluctuation effects in optic nerve of *Rana pipiens*. *Journal of General Physiology, 66*, 583–616.

Croner, L. J., Purpura, K., & Kaplan, E. (1993). Response variability in retinal ganglion cells of primates. *Proceedings of the National Academy of Science USA, 90*, 8128–8130.

Foley, J. M. (1994). Human luminance pattern vision mechanisms: masking experiments require a new model. *Journal of the Optical Society of America A, 11*, 1710–1719.

Foley, J. M., & Legge, G. E. (1981). Contrast detection and near-threshold discrimination in human vision. *Vision Research, 21*, 1041–1053.

Geisler, W. S., & Albrecht, D. G. (1997). Visual cortex neurons in monkeys and cats: detection, discrimination, and identification. *Visual Neuroscience, 14*, 897–919.

Gorea, A., & Sagi, D. (2001). Disentangling signal from noise in visual contrast discrimination. *Nature Neuroscience, 4*, 1146–1150.

Gottesman, J., Rubin, G. S., & Legge, G. E. (1981). A power law for perceived contrast in human vision. *Vision Research, 21*, 791–799.

Green, D. M., & Swets, J. A. (1966). *Signal detection theory and psychophysics*. New York: Wiley.

Greenlee, M. W., & Heitger, F. (1988). The functional role of contrast adaptation. *Vision Research, 28*, 791–797.

Heeger, D. J. (1992). Half-squaring in responses of cat striate cells. *Visual Neuroscience, 9*, 427–443.

Jagadeesh, B., Wheat, H. S., Kontsevich, L. L., Tyler, C. W., & Ferster, D. (1997). Direction selectivity of synaptic potentials in simple cells of the cat visual cortex. *Journal of Neurophysiology, 78*, 2772–2789.

Kontsevich, L. L. (1995). The nature of the inputs to cortical motion detectors. *Vision Research, 35*, 2785–2793.

Kontsevich, L. L., Chen, C.-C., Verghese, P., & Tyler, C. W. (in press). A critical look at the unique criterion constraint. *Nature Neuroscience*.

Kulikowski, J. J., & Gorea, A. (1978). Complete adaptation to patterned stimuli: a necessary and sufficient condition for Weber's law for contrast. *Vision Research, 18*, 1223–1227.

Lasley, D. J., & Cohn, T. E. (1981). Why luminance discrimination may be better than detection. *Vision Research, 20*, 273–278.

Legge, G. E. (1981). A power law for contrast discrimination. *Vision Research, 21*, 457–467.

Legge, G. E. (1984). Binocular contrast summation. II. Quadratic summation. *Vision Research, 24*, 385–394.

Legge, G. E., & Foley, J. M. (1980). Contrast masking in human vision. *Journal of the Optical Society of America, 70*, 458–471.

Legge, G. E., Kersten, D., & Burgess, A. E. (1987). Contrast discrimination in noise. *Journal of the Optical Society of America A, 4*, 391–404.

Lu, Z. L., & Dosher, B. A. (1999). Characterizing human perceptual inefficiencies with equivalent internal noise. *Journal of the Optical Society of America A, 16*, 764–778.

Manahilov, V., & Simpson, W. (1999). Energy model for contrast detection: spatiotemporal characteristics of threshold vision. *Biological Cybernetics, 81*, 61–71.

Nachmias, J., & Sansbury, R. V. (1974). Letter: Grating contrast: discrimination may be better than detection. *Vision Research, 14*, 1039–1042.

Pelli, D. G. (1985). Uncertainty explains many aspects of visual contrast detection and discrimination. *Journal of the Optical Society of America A, 2*, 1508–1532.

Pelli, D. G. (1991). Noise in the visual system may be early. In M. S. Landy, & J. A. Movshon (Eds.), *Computational model of visual processing* (pp. 147–151). Cambridge: MIT Press.

Pelli, D. G., & Zhang, L. (1991). Accurate control of contrast on microcomputer displays. *Vision Research, 31*, 1337–1350.

Ross, J., & Speed, H. D. (1991). Contrast adaptation and contrast masking in human vision. *Proceeding of the Royal Society of London, B246*, 61–69.

Ross, J., Speed, H. D., & Morgan, M. J. (1993). The effects of adaptation and masking on incremental thresholds for contrast. *Vision Research, 33*, 2051–2056.

Sclar, G., Maunsell, J. H. R., & Lennie, P. (1990). Coding of image contrast in central visual pathways of the macaque monkey. *Vision Research, 30*, 1–10.

Snowden, R. J., Treue, S., & Andersen, R. A. (1992). The response of neurons in areas V1 and MT of the alert rhesus monkey to moving random dot patterns. *Experimental Brain Research, 88*, 389–400.

Softky, W. R., & Koch, C. (1993). The highly irregular firing of cortical cells is inconsistent with temporal integration of random EPSPs. *Journal of Neuroscience, 13*, 334–350.

Solomon, J. A., & Pelli, D. G. (1994). The visual filter mediating letter identification. *Nature, 369*, 395–397.

Stevens, S. S. (1957). On the psychophysical law. *Psychological Review, 64*, 153–181.

Stromeyer, C. F., & Klein, S. (1974). Spatial frequency channels in human vision as asymmetric (edge) mechanisms. *Vision Research, 14*, 1409–1420.

Swets, J. A. (1961). Is there a sensory threshold? *Science, 134*, 168–177.

Tanner, W. P., Jr. (1961). Physiological implications of psychophysical data. *Annals of the New York Academy of Sciences, 89*, 752–765.

Tanner, W. P., Jr.,, & Birdsall, T. G. (1958). Definition of d' and η as psychophysical measures. *Journal of Acoustic Society of America, 30*, 922–928.

Thomas, J. P., & Olzak, L. A. (1997). Contrast gain control and fine spatial discriminations. *Journal of Optical Society of America A, 14*, 2392–2405.

Tolhurst, D. J., Movshon, J. A., & Dean, A. F. (1983). The statistical reliability of signals in single neurons in cat and monkey visual cortex. *Vision Research, 23*, 775–785.

Tyler, C. W., & Chen, C. (2000). Signal detection theory in the 2AFC paradigm: attention, channel uncertainty and probability summation. *Vision Research, 40*, 3121–3144.

Tyler, C. W., & Liu, L. (1996). Saturation revealed by clamping the gain of the retinal light response. *Vision Research, 36*, 2553–2562.

Vogels, R., Spileers, W., & Orban, G. A. (1989). The response variability of striate cortical neurons in the behaving monkey. *Experimental Brain Research, 77*, 432–436.

Watson, A. B. (2000). Visual detection of spatial contrast patterns: evaluation of five simple models. *Optics Express, 6*, 12–33.

Watson, A. B., & Solomon, J. A. (1999). ModelFest data: fit of the Watson–Solomon model. *Investigative Ophthalmology and Visual Science, 40*, S572.

Wilson, H. R. (1980). A transducer function for threshold and suprathreshold human vision. *Biological Cybernetics, 38*, 171–178.

Wilson, H. R., & Humanski, R. (1993). Spatial frequency adaptation and contrast gain control. *Vision Research, 33*, 1133–1149.

Wilson, H. R., McFarlane, D. K., & Phillips, G. C. (1983). Spatial frequency tuning of orientation selective units estimated by oblique masking. *Vision Research, 23*, 873–882.